

Article

Nor-24-homoscalaranes, Neutrophilic Inflammatory Mediators from the Marine Sponge *Lendenfeldia* sp.

Bo-Rong Peng¹ , Li-Guo Zheng^{2,3}, Lo-Yun Chen^{1,4} , Mohamed El-Shazly⁵, Tsong-Long Hwang^{6,7,8,9,10} , Jui-Hsin Su^{3,11}, Mei-Hsien Lee^{1,4,12} , Kuei-Hung Lai^{1,4,13,*}  and Ping-Jyun Sung^{3,11,14,15,16,*} 

- ¹ Graduate Institute of Pharmacognosy, College of Pharmacy, Taipei Medical University, Taipei 110301, Taiwan; peng_br@tmu.edu.tw (B.-R.P.); m303110004@tmu.edu.tw (L.-Y.C.); lmh@tmu.edu.tw (M.-H.L.)
 - ² Doctoral Degree Program in Marine Biotechnology, National Sun Yat-sen University, Kaohsiung 804201, Taiwan; t0919928409@gmail.com
 - ³ National Museum of Marine Biology and Aquarium, Pingtung 944401, Taiwan; x2219@nmmba.gov.tw
 - ⁴ PhD Program in Clinical Drug Development of Herbal Medicine, College of Pharmacy, Taipei Medical University, Taipei 110301, Taiwan
 - ⁵ Department of Pharmacognosy, Faculty of Pharmacy, Ain-Shams University, Organization of African Unity Street, Abassia, Cairo 11566, Egypt; mohamed.elshazly@pharma.asu.edu.eg
 - ⁶ Research Center for Chinese Herbal Medicine, College of Human Ecology, Chang Gung University of Science and Technology, Taoyuan 333324, Taiwan; htl@mail.cgu.edu.tw
 - ⁷ Graduate Institute of Health Industry Technology, College of Human Ecology, Chang Gung University of Science and Technology, Taoyuan 333324, Taiwan
 - ⁸ Graduate Institute of Natural Products, College of Medicine, Chang Gung University, Taoyuan 333323, Taiwan
 - ⁹ Department of Chemical Engineering, Ming Chi University of Technology, New Taipei City 243303, Taiwan
 - ¹⁰ Department of Anesthesiology, Chang Gung Memorial Hospital, Taoyuan 333423, Taiwan
 - ¹¹ Department of Marine Biotechnology and Resources, National Sun Yat-sen University, Kaohsiung 804201, Taiwan
 - ¹² Center for Reproductive Medicine and Sciences, Taipei Medical University Hospital, Taipei 110301, Taiwan
 - ¹³ Traditional Herbal Medicine Research Center, Taipei Medical University Hospital, Taipei 110301, Taiwan
 - ¹⁴ Graduate Institute of Natural Products, Kaohsiung Medical University, Kaohsiung 807378, Taiwan
 - ¹⁵ Chinese Medicine Research and Development Center, China Medical University Hospital, Taichung 404394, Taiwan
 - ¹⁶ PhD Program in Pharmaceutical Biotechnology, Fu Jen Catholic University, New Taipei City 242062, Taiwan
- * Correspondence: kueihunglai@tmu.edu.tw (K.-H.L.); pjsung@nmmba.gov.tw (P.-J.S.); Tel.: +886-2-2736-1661 (ext. 6157) (K.-H.L.); +886-8-882-5087 (P.-J.S.)



Citation: Peng, B.-R.; Zheng, L.-G.; Chen, L.-Y.; El-Shazly, M.; Hwang, T.-L.; Su, J.-H.; Lee, M.-H.; Lai, K.-H.; Sung, P.-J. Nor-24-homoscalaranes, Neutrophilic Inflammatory Mediators from the Marine Sponge *Lendenfeldia* sp. *Pharmaceuticals* **2023**, *16*, 1258. <https://doi.org/10.3390/ph16091258>

Academic Editor: María J. Ortega

Received: 20 July 2023

Revised: 28 August 2023

Accepted: 4 September 2023

Published: 6 September 2023



Copyright: © 2023 by the authors. Licensee MDPI, Basel, Switzerland. This article is an open access article distributed under the terms and conditions of the Creative Commons Attribution (CC BY) license (<https://creativecommons.org/licenses/by/4.0/>).

Abstract: The marine sponge *Lendenfeldia* sp., collected from the Southern waters of Taiwan, was subjected to chemical composition screening, resulting in the isolation of four new 24-homoscalarane compounds, namely lendenfeldaranes R–U (1–4). The structures and relative stereochemistry of the new metabolites 1–4 were assigned based on NMR studies. The absolute configurations of compounds 1–4 were determined by comparing the calculated and experimental values of specific optical rotation. The antioxidant and anti-inflammatory activities of the isolated compounds were assayed using superoxide anion generation and elastase release assays. These assays are used to determine neutrophilic inflammatory responses of respiratory burst and degranulation. Compounds 2 and 4 inhibited superoxide anion generation by human neutrophils in response to formyl-L-methionyl-L-leucyl-L-phenylalanine/cytochalasin B (fMLP/CB) with IC₅₀: 3.98–4.46 μM. Compounds 2 and 4 inhibited fMLP/CB-induced elastase release, with IC₅₀ values ranging from 4.73 to 5.24 μM. These findings suggested that these new 24-homoscalarane compounds possess unique structures and potential anti-inflammatory activity.

Keywords: marine sponge; *Lendenfeldia* sp.; scalarane; anti-inflammatory; neutrophil

1. Introduction

Marine sponges belonging to the genus *Lendenfeldia* (phylum Porifera, class Demospongia, subclass Keratosa, order Dictyoceratida, family Thorectidae) are widely distributed in the flat reefs of the Asia-Pacific region. These sponges can also be found in aquarium tanks and are considered pests as they can proliferate in aquacultures even under standard conditions [1]. Previous research on *Lendenfeldia* sponges revealed a rich diversity of secondary metabolites, with sesterterpenoids being particularly prominent [2–9]. These sesterterpenoids exhibit a broad spectrum of biological activities, including cytotoxicity [10–31], anti-inflammatory properties [5,7,18,32–36], anti-HIV effects [3,37], antimicrobial [15,16,22,38–41] and anti-neurofibroma activity [42]. Anti-neutrophil inflammatory agents refer to substances that aim to reduce or inhibit the inflammatory response mediated by neutrophils. Neutrophils are a type of white blood cell that are essential to the immune response. They play a crucial role in the initial response to infection and tissue injury [43]. While neutrophils are important for combating pathogens and promoting tissue repair, their excessive or prolonged activation can lead to harmful inflammation and tissue damage. Therefore, targeting neutrophil-mediated inflammation is an area of interest in various inflammatory conditions, including autoimmune diseases, acute respiratory distress syndrome (ARDS), and inflammatory bowel disease (IBD) [44]. In our two previous reports, we isolated a series of scalarane-type sesterterpenoids from the marine sponge *Lendenfeldia* sp. and tested their anti-inflammatory activity against superoxide anion generation and elastase release, which represented the neutrophilic inflammatory responses of respiratory burst and degranulation, respectively. The results indicated that the potent activity of this class of compounds could lead to their further development as anti-neutrophilic agents [5,7]. In our ongoing investigation, aiming to discover new metabolites from *Lendenfeldia* sp., we identified four novel 24-homoscalarane-type sesterterpenoids named lendenfeldaranes R–U (1–4) (Figure 1). The determination of the structures of compounds 1–4 involved a thorough analysis of their Infrared (IR), Specific Optical Rotation (SOR), Mass (MS), and Nuclear Magnetic Resonance (NMR) spectra. Moreover, their NMR data were compared with those of known compounds with structural similarities. To establish the absolute configuration of compounds 1–4, we compared the experimental optical rotation with the calculated optical rotation spectra. Additionally, we evaluated the anti-inflammatory activity of these compounds by assessing their ability to inhibit superoxide anion generation and elastase release in N-formyl-methionyl-leucyl phenylalanine/cytochalasin B (fMLF/CB)-induced human neutrophils.

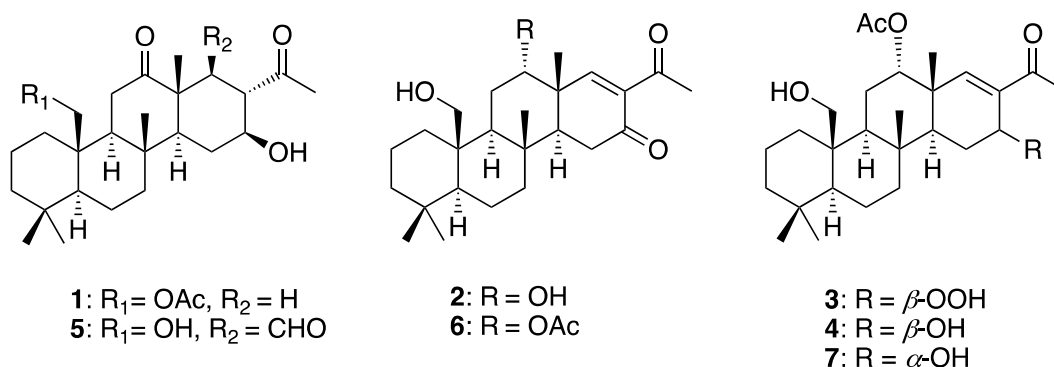


Figure 1. The identified 24-homoscalaranes from the marine sponge *Lendenfeldia* sp.

2. Results and Discussion

Compound 1 was obtained as a white powder, and its molecular formula was determined as C₂₇H₄₂O₅ based on the presence of a sodium adduct at *m/z* 469.29256 in HRESIMS (calculated for C₂₇H₄₂O₅ + Na, 469.29245) and ¹³C NMR data (Table 1). The IR spectrum of 1 exhibited characteristic peaks indicating the presence of ketone carbonyl (ν_{\max} 1703 cm⁻¹), ester carbonyl (ν_{\max} 1736 cm⁻¹), and hydroxy (ν_{\max} 3429 cm⁻¹) func-

tional groups. The ^1H NMR spectroscopic data of **1** (Table 1) revealed six methyl groups at δ_{H} 0.85, 0.88, 1.13, 1.26, 2.06, and 2.19 (each 3H, singlet), and one oxymethine proton at δ_{H} 3.80 (1H, triple doublet, $J = 9.6, 9.6, 3.2$ Hz). The presence of an oxymethylene group was indicated by the anisochronous signals of the geminal protons observed at δ_{H} 4.67 (1H, doublet, $J = 12.4$ Hz) and 4.21 (1H, doublet of doublets, $J = 12.4, 1.2$ Hz). An analysis of the HSQC and ^{13}C spectroscopic data revealed that compound **1** consists of 27 carbon atoms, including six methyl groups, nine sp^3 methylene groups (including one oxymethylene), five sp^3 methine groups (including one oxymethine), four sp^3 quaternary carbons, and three sp^2 quaternary carbons (including three carbonyls). Based on the ^1H and ^{13}C NMR spectroscopic data, compound **1** was found to possess an acetoxy group (δ_{H} 2.06, 3H, singlet; δ_{C} 170.8, carbonyl; 21.1, methyl) and two ketone carbonyls (δ_{C} 212.4, carbonyl; 214.4, carbonyl), accounting for three degrees of unsaturation. The remaining four degrees of unsaturation indicated that compound **1** possesses a tetracyclic structure.

To gain a more comprehensive understanding of the structure of **1**, 2D NMR spectra, including ^1H – ^1H correlation spectroscopy (COSY) and heteronuclear multiple-bond coherence (HMBC) spectra were employed. These spectra were used to analyze the correlations between protons (^1H) and neighboring atoms, as well as the connectivity of multiple bonds between different nuclei (Figure 2). The ^1H – ^1H COSY cross-peaks revealed four distinct proton spin systems: H-5/H₂-6/H₂-7, H₂-1/H₂-2/H₂-3, H-9/H₂-10, and H-14/H₂-15/H₂-16/H-17/H₂-18. The HMBC cross-signals between H₃-21 and C-7, C-8, C-9, C-14; H₃-20 and C-3, C-4, C-5, C-19; H₂-22 and C-1, C-9, the ester carbonyl (δ_{C} 170.8); H₃-23 and C-12, C-13, C-14, C-18; H₃-25 and C-17, C-24; H₂-11 and C-12 established connections between the partial structures. A comparison with the previous literature aided in successfully constructing the overall structure of **1**. The obtained data showed similarities to a known 24-homescalarane compound, felixin F (**5**) [45]. However, notable differences were observed between compounds **1** and **5**. In compound **5**, the hydroxy group at C-22 (δ_{H} 3.93, 1H, doublet, $J = 11.6$ Hz; 4.07, 1H, doublet, $J = 11.6$ Hz; δ_{C} 62.7) was replaced by an acetoxy group in compound **1** (δ_{H} 4.67, 1H, doublet, $J = 12.4$ Hz; 4.21, 1H, doublet of doublets, $J = 12.4, 1.2$ Hz; δ_{C} 64.5). Additionally, **1** lacked the aldehyde group present in compound **5**, which was substituted by a methylene carbon.

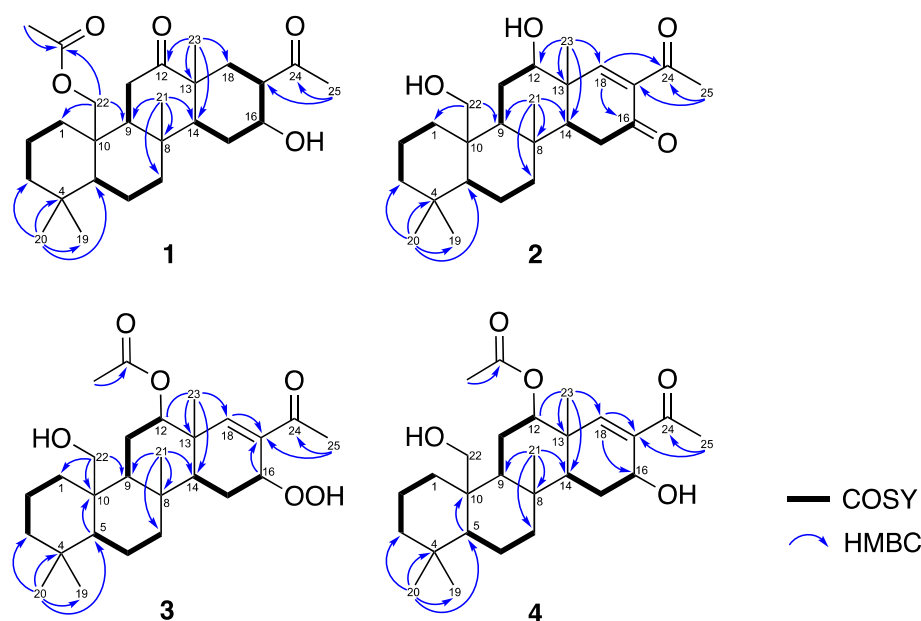


Figure 2. Key 2D correlations of planar structures of **1**–**4**.

Through a literature search, it was found that all naturally occurring scalaranes exhibit β -oriented methyl groups (Me-23 and Me-22) at C-13 and C-10, respectively, regardless of their oxidation state ($-\text{CH}_2\text{OH}$, $-\text{CH}_2\text{OAc}$, $-\text{COOH}$, and $-\text{CHO}$) [7]. The orientations

of these methyl groups remained consistent within the carbon skeleton, with C-13 and C-10 serving as anchor points for analysis. The relative configuration of **1** was established through NOESY experiments (Figure 3). The NOESY interactions between H₃-23 and H-17, as well as H₃-21, and between H₂-22 and H₃-20, and H₃-21, revealed the β-orientation of H₃-23, H₂-22, H₃-21, H₃-20, and H-17. An interaction between H-5 and H-9 indicated their spatial proximity. A further correlation analysis showed a correlation between H-9 and H-14, as well as a correlation between H-14 and H-16, suggesting an α-orientation for H-5, H-9, H-14, and H-16. Based on these findings, the structure of **1** was determined, and the assigned stereogenic centers were identified as (5*S**,8*R**,9*S**,10*R**,13*R**,14*S**,16*S**,17*S**).

Table 1. The NMR data for compounds **1** and **2**.

C/H	1		2	
	δ_{H} (J in Hz) ^a	δ_{C} (mult.) ^b	δ_{H} (J in Hz) ^c	δ_{C} (mult.) ^d
1	2.00 m; 0.77 ddd (12.4, 12.4, 4.4) ^e	34.3, CH ₂ ^f	2.13 m; 0.73 ddd (12.0, 12.0, 3.0) ^e	34.1, CH ₂ ^f
2	1.61 m; 1.48 m	17.9, CH ₂	1.56 m; 1.37 m	17.7, CH ₂
3	1.45 m; 1.17 m	41.4, CH ₂	1.43 m; 1.19 m	41.7, CH ₂
4		33.0, C		33.0, C
5	1.00 m	56.8, CH	1.03 dd (12.6, 2.4)	56.9, CH
6	1.61 m	18.2, CH ₂	1.49 m	18.4, CH ₂
7	1.95 m; 1.15 m	41.5, CH ₂	1.77 ddd (12.6, 3.0, 3.0); 1.08 m	41.1, CH ₂
8		37.2, C		37.3, C
9	1.32 m	60.2, CH	1.52 m	51.8, CH
10		41.0, C		41.8, C
11	3.97 dd (14.4, 14.4) 2.50 dd (14.4, 2.8)	37.6, CH ₂	2.32 m; 1.86 ddd (16.2, 2.4, 2.4)	28.3, CH ₂
12		214.4, C	3.98 br s	73.9, CH
13		48.5, C		42.6, C
14	1.19 m	55.9, CH	2.14 m	47.5, CH
15	1.98 m; 1.57 m	27.6, CH ₂	2.53 m; 2.24 m	34.9, CH ₂
16	3.80 ddd (9.6, 9.6, 3.2)	70.9, CH		198.2, C
17	2.49 m	53.7, CH		142.8, C
18	2.05 m	36.8, CH	7.55 s	165.9, CH
19	0.88 s	33.7, CH ₃	0.86 s	33.9, CH ₃
20	0.85 s	21.8, CH ₃	0.77 s	21.8, CH ₃
21	1.13 s	16.0, CH ₃	1.11 s	15.8, CH ₃
22	4.67 d (12.4) 4.21 dd (12.4, 1.2)	64.5, CH ₂	4.06 d (11.4); 3.09 dd (11.4)	62.8, CH ₂
23	1.26 s	19.3, CH ₃	1.11 s	18.6, CH ₃
24		212.4, C		198.3, C
25	2.19 s	28.8, CH ₃	2.45 s	30.7, CH ₃
22-OAc	2.06 s	170.8, C 21.1, CH ₃		

^a Spectra recorded at 400 MHz in CDCl₃; ^b spectra recorded at 100 MHz in CDCl₃; ^c spectra recorded at 600 MHz in CDCl₃; ^d spectra recorded at 150 MHz in CDCl₃; ^e J values (in Hz) in parentheses; ^f attached protons were deduced by the HSQC experiment.

To determine the absolute stereochemistry of **1**, two possible configurations were considered: **1-5*S*,8*R*,9*S*,10*R*,13*R*,14*S*,16*S*,17*S***, and **1-5*R*,8*S*,9*R*,10*S*,13*S*,14*R*,16*R*,17*R***. These configurations were fed into Gaussian 16 software to calculate the conformation, optimize the structure, and determine the specific optical rotation (SOR) values (Table 2). The calculated SOR value of **1-5*S*,8*R*,9*S*,10*R*,13*R*,14*S*,16*S*,17*S*** (+31) was consistent with the experimental result of compound **1** (positive). Based on these results, the configurations of the stereogenic centers in **1** were determined to be (5*S*,8*R*,9*S*,10*R*,13*R*,14*S*,16*S*,17*S*). Consequently, the structure of **1** was identified as a new sesterterpenoid and named lendenfeldarane R.

Table 2. The NMR data for compounds **3** and **4**.

C/H	3		4	
	δ_{H} (J in Hz) ^a	δ_{C} (mult.) ^b	δ_{H} (J in Hz) ^c	δ_{C} (mult.) ^d
1	2.08 m; 0.58 ddd (13.2, 13.2, 2.8) ^e	34.1, CH ₂ ^f	2.07 m; 0.56 ddd (12.0, 12.0, 3.0) ^e	34.2, CH ₂ ^f
2	1.58 m	17.8, CH ₂	1.56 m	17.9, CH ₂
3	1.41 m; 1.17 m	41.8, CH ₂	1.44 m; 1.17 m	41.7, CH ₂
4		33.0, C		33.0, C
5	1.02 m	56.8, CH	0.99 dd (12.6, 2.4)	57.0, CH
6	1.56 m; 1.45 m	18.3, CH ₂	1.58 m; 1.52 m	18.4, CH ₂
7	1.91 m; 1.18 m	41.2, CH ₂	1.92 m; 1.03 m	41.4, CH ₂
8		36.8, C		37.2, C
9	1.41 m	53.5, CH	1.33 m	53.5, CH
10		41.8, C		41.8, C
11	2.35 m; 1.46 m	21.9, CH ₂	1.91 m; 2.25 m	25.1, CH ₂
12	4.97 d (2.8)	76.2, CH	4.96 dd (2.8, 2.8)	76.6, CH
13		41.7, C		41.6, C
14	1.86 dd (13.2, 2.0)	43.6, CH	1.50 m	47.5, CH
15	1.92 m; 2.29 m	25.2, CH ₂	2.14 m; 1.50 m	25.7, CH ₂
16	4.91 dd (4.0, 1.6)	77.2, CH	4.61 dd (8.8, 6.6)	68.1, CH
17		133.6, C		132.4, C
18	6.73 s	155.7, CH	6.59 s	152.4, CH
19	0.85 s	33.8, CH ₃	0.88 s	33.8, CH ₃
20	0.77 s	21.9, CH ₃	0.76 s	21.9, CH ₃
21	1.09 s	16.6, CH ₃	1.10 s	16.4, CH ₃
22	4.05 d (11.6); 3.91 dd (11.6)	62.8, CH ₂	4.27 d (11.4); 3.90 dd (11.4)	62.7, CH ₂
23	1.06 s	19.4, CH ₃	1.20 s	20.9, CH ₃
24		199.3, C		202.1, C
25	2.25 s	25.8, CH ₃	2.25 s	25.7, CH ₃
12-OAc		170.8, C		170.6, C
	2.03 s	21.3, CH ₃	2.04 s	21.3, CH ₃
16-OOH	9.27 s			

^a Spectra recorded at 400 MHz in CDCl₃; ^b spectra recorded at 100 MHz in CDCl₃; ^c spectra recorded at 600 MHz in CDCl₃; ^d spectra recorded at 150 MHz in CDCl₃; ^e *J* values (in Hz) in parentheses; ^f attached protons were deduced by the HSQC experiment.

Compound **2** was discovered to have the molecular formula C₂₅H₃₈O₄, which was determined from a (+)-HRESIMS signal at *m/z* 425.26645 (calculated for C₂₅H₃₈O₄+Na, 425.26623) and ¹³C data indicating the presence of seven unsaturated degrees. The IR spectrum of **2** showed absorption peaks for carbonyl groups (ν_{max} 1707 cm⁻¹ and 1676 cm⁻¹) and a hydroxy group (ν_{max} 3417 cm⁻¹). Analyzing the 1D NMR data (Table 2), it was found that compound **2** was similar to felixin B (**6**) [46], with the main difference being the presence of a functional group at C-12. In compound **2**, the chemical shift of H-12 (δ_{H} 3.98, 1H, br s) was shifted downfield compared to its counterpart in felixin B (**6**) (δ_{H} 4.97, 1H, dd, *J* = 2.8, 2.8 Hz). The absence of acetoxy signals suggested that felixin B (**6**) was the 12-acetyl derivative of compound **2**. Further confirmation of the planar structure of compound **2** was obtained through the interpretation of 2D NMR spectroscopic data (Figure 2). The correlations observed among the chiral centers in the core rings A-D of **2** were identical to those observed in **1**. In the NOESY experiment of **2** (Figure 3), the α -orientation of the hydroxy group at C-12 was determined based on the NOESY correlation between H-12 and H₃-23. As a result, the configurations of the stereogenic carbons in **2** were established as (5*S**, 8*R**, 9*S**, 10*R**, 12*S**, 13*R**, 14*S**). The SOR was employed to determine the absolute configuration of **2**. The calculated SOR values for 2-5*S*, 8*R*, 9*S*, 10*R*, 12*S*, 13*R*, 14*S* and 2-5*R*, 8*S*, 9*R*, 10*S*, 12*R*, 13*S*, 14*R* were positive (78) and negative (−78), respectively (Table 2). The experimental SOR data of **2** (positive) matched with the configuration 2-5*S*, 8*R*, 9*S*, 10*R*, 12*S*, 13*R*, 14*S*. Based on the aforementioned analyses, the structure of **2** was successfully determined, leading to its identification and designation as lendenfeldarane **S**.

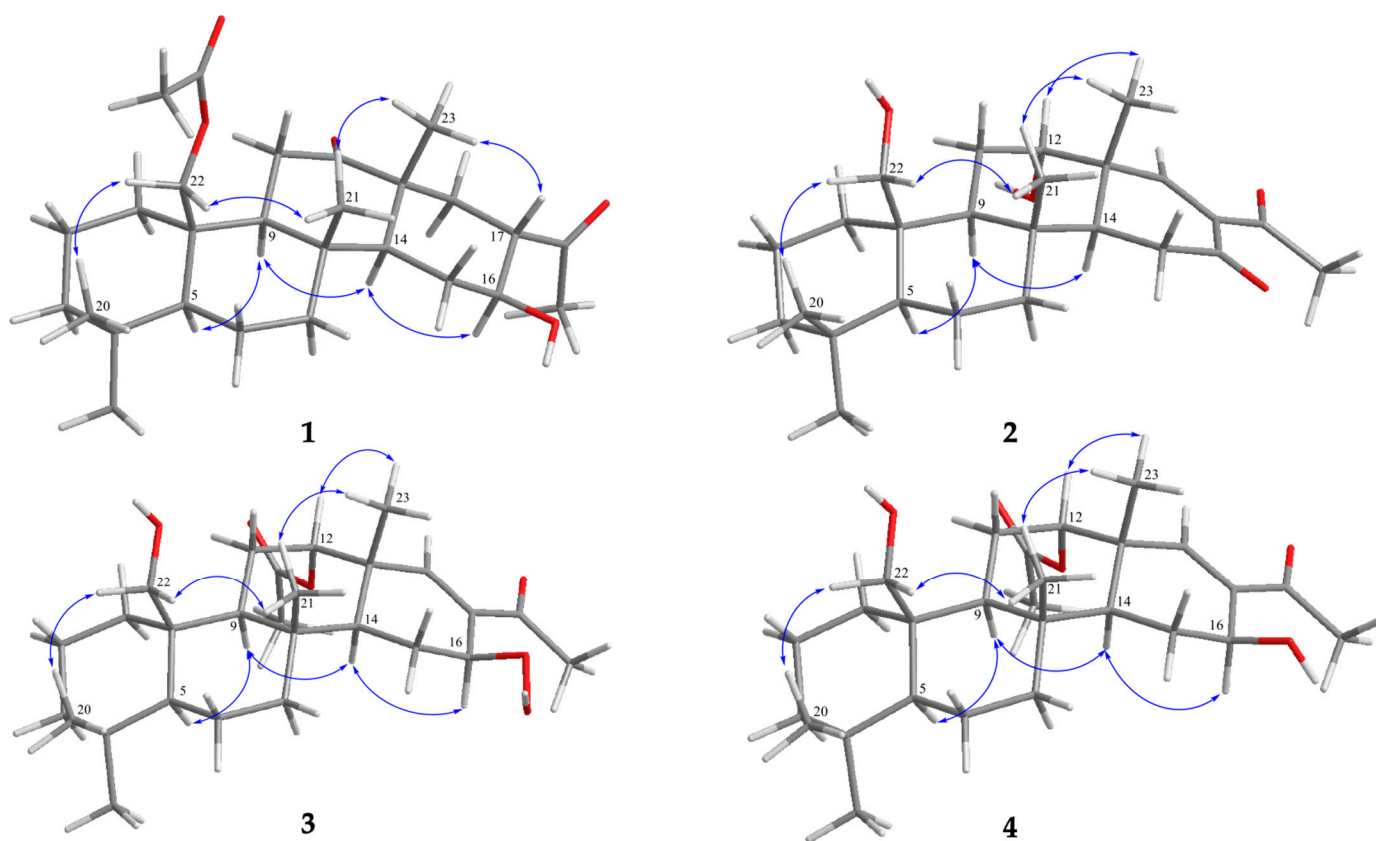


Figure 3. Selective NOESY correlations (\curvearrowright) of relative structures of 1–4.

Compound **3** was acquired in the form of a white powder, and its molecular formula was determined as $C_{27}H_{42}O_6$ based on the HRESIMS signal at m/z 485.28737 $[M + Na]^+$ (calculated for $C_{27}H_{42}O_6 + Na$, 485.28736) and ^{13}C data suggesting the presence of seven degrees of unsaturation. The IR spectrum of **3** exhibited prominent peaks at ν_{max} 3459, 1727, and 1666, indicating the presence of hydroxy, ester, and α,β -unsaturated ketone groups, respectively. Analysis of the 1H and ^{13}C NMR spectroscopic data (Table 3) revealed the presence of an acetoxy group (δ_H 2.03, 3H, s; δ_C 170.8, C; 21.3, CH_3) and a ketonic carbonyl group (δ_C 199.3) within compound **3**. Moreover, the ^{13}C resonances at δ_C 133.6 (C) and 155.7 (CH) suggested the existence of a trisubstituted olefin, accounting for three degrees of unsaturation. Compound **3** was identified as an analog of tetracyclic sesterterpenoid. The NMR data resembled those of felixin C (**7**) [46]. The chemical shift of H-16 in felixin C (**7**) (δ_H 4.55, d, $J = 4.8$ Hz) was shifted downfield in **3** (δ_H 4.91, dd, $J = 4.0, 1.6$ Hz), with an additional signal for a hydroperoxide group (δ_H 9.27, 1H, s). The presence of a hydroperoxide group substitution at position 16 was deduced from the HMBC cross-peak (Figure 2) between H-16 and C-14, C-17, C-18, and from H-14 to C-16, as well as from the COSY correlation between H-15, H-14, and H-16. Additionally, comparing the ^{13}C NMR data with those of **1** and **4**, the C-16 carbon resonating at δ_C 77.2 in **3** was more downfield than δ_C 70.9 in **1** and δ_C 68.1 in **4**, revealing that the hydroperoxide group was located at C-16 position.

Table 3. Experimental and calculated specific optical rotation values of 1–4.

	Cald. Value ^a	Exp. Value
Exp. 1 ^b		21
Cald. 1-5 <i>S</i> ,8 <i>R</i> ,9 <i>S</i> ,10 <i>R</i> ,13 <i>R</i> ,14 <i>S</i> ,16 <i>S</i> ,17 <i>S</i>	31	
Cald. 1-5 <i>R</i> ,8 <i>S</i> ,9 <i>R</i> ,10 <i>S</i> ,13 <i>S</i> ,14 <i>R</i> ,16 <i>R</i> ,17 <i>R</i>	−31	
Exp. 2 ^c		61
Cald. 2-5 <i>S</i> ,8 <i>R</i> ,9 <i>S</i> ,10 <i>R</i> ,12 <i>S</i> ,13 <i>R</i> ,14 <i>S</i>	78	
Cald. 2-5 <i>R</i> ,8 <i>S</i> ,9 <i>R</i> ,10 <i>S</i> ,12 <i>R</i> ,13 <i>S</i> ,14 <i>R</i>	−78	
Exp. 3 ^d		41
Cald. 3-5 <i>S</i> ,8 <i>R</i> ,9 <i>S</i> ,10 <i>R</i> ,12 <i>S</i> ,13 <i>R</i> ,14 <i>S</i> ,16 <i>S</i>	15	
Cald. 3-5 <i>R</i> ,8 <i>S</i> ,9 <i>R</i> ,10 <i>S</i> ,12 <i>R</i> ,13 <i>S</i> ,14 <i>R</i> ,16 <i>R</i>	−15	
Exp. 4 ^e		76
Cald. 4-5 <i>S</i> ,8 <i>R</i> ,9 <i>S</i> ,10 <i>R</i> ,12 <i>S</i> ,13 <i>R</i> ,14 <i>S</i> ,16 <i>S</i>	103	
Cald. 4-5 <i>R</i> ,8 <i>S</i> ,9 <i>R</i> ,10 <i>S</i> ,12 <i>R</i> ,13 <i>S</i> ,14 <i>R</i> ,16 <i>R</i>	−103	

^a Solvent phase in CHCl₃; ^b $[\alpha]_D^{25}$ (c 0.025, CHCl₃); ^c $[\alpha]_D^{25}$ (c 0.065, CHCl₃); ^d $[\alpha]_D^{25}$ (c 0.045, CHCl₃); ^e $[\alpha]_D^{25}$ (c 0.105, CHCl₃).

Further insights into the structure of **3** were obtained through the NOESY experiment (Figure 3). The observed correlations provided valuable information regarding the configurations of the chiral centers in the core rings A–C of **3**, which were found to be identical to those observed in **1**. Notably, H₃–23 showed NOE correlations with H₃–21 and H-12, indicating the β-orientation of H-12. Additionally, H-14 displayed NOE correlations with H-9 and H-16, indicating the β-orientation of the hydroperoxide group at C-16. To determine the absolute configuration of **3**, a comparison was made between its experimental optical rotation and the corresponding SOR value. The calculated SOR values for 3-5*S*,8*R*,9*S*,10*R*,12*S*,13*R*,14*S*,16*S* and 3-5*R*,8*S*,9*R*,10*S*,12*R*,13*S*,14*R*,16*R* were positive (15) and negative (−15), respectively (Table 2). The experimental SOR data of **3** (positive) matched with the configuration 3-5*S*,8*R*,9*S*,10*R*,12*S*,13*R*,14*S*,16*S*. Based on the aforementioned results, the structure of **3** was determined and assigned the name lendenfeldarane T.

Compound **4** was obtained in the form of an unstructured fine powder. Its molecular formula was determined to be C₂₇H₄₂O₅ based on the (+)-HRESIMS pseudo-molecular ion peak at *m/z* 469.29221 (calculated for C₂₇H₄₂O₅+Na, 469.29245) and ¹³C data, which indicated the presence of seven degrees of unsaturation. The IR spectrum of **4** exhibited absorption bands corresponding to hydroxy groups (maximum absorption at 3486 cm^{−1}), ester carbonyl groups (maximum absorption at 1726 cm^{−1}), and α,β-unsaturated ketone groups (maximum absorption at 1655 cm^{−1}). The structure of **4** was determined through the analysis of 1D and 2D NMR spectroscopic data (refer to Table 3). Based on these findings, it was observed that the overall structure of **4** closely resembled that of felixin B (**7**) [46]. The ¹³C and ¹H NMR data of **4** were similar to those of compound **7**, except for carbon resonances at C-16 and C-17, which appeared at δ_C 63.3 (CH) and 138.2 (C) in compound **7** and at δ_C 68.1 (CH) and 134.2 (C) in **4**, indicating that **4** was the 16*S* isomer of compound **7**. Analysis of the NOESY spectra (refer to Figure 3) revealed a cross-peak from H-14 to H-16, indicating an α-orientation of H-16 in **4**. According to the above data, the structure of **4** was determined, and the compound was named lendenfeldarane U.

N-formyl-methionyl-leucyl-phenylalanine (fMLF) and pathogen-associated molecular patterns (PAMPs) can stimulate neutrophils, leading to the initiation of inflammatory responses such as the generation of O₂^{•−} (respiratory burst) and the release of elastase (degranulation) [7]. To evaluate the anti-inflammatory properties of nor-24-homoscalaranes, all the isolated compounds were tested on fMLF-induced human neutrophils, and the findings are summarized in Table 4. As a positive control, LY294002, a phosphoinositide 3-kinase (PI3K) inhibitor, was employed, given the established role of PI3K in regulating neutrophil respiratory burst and/or degranulation [47,48]. Compounds **2** and **4** demonstrated significant activity against both O₂^{•−} accumulation (IC₅₀ = 3.98–4.46 μM) and elastase release (IC₅₀ = 4.73–5.24 μM). On the other hand, compounds **1** and **3** were inactive at a concentration of 10 μM. These results emphasized the importance of the conjugated

functionality at C-17-18-24 for anti-inflammatory activity, while the substitution of the peroxy group at C-16 may diminish this effect.

Table 4. Effect of compounds 1–4 on superoxide anion generation and elastase release in fMLF/CB-induced human neutrophils.

Compounds	Superoxide Anion Generation			Elastase Release		
	IC ₅₀ (μM)	Inh%		IC ₅₀ (μM)	Inh%	
1		9.19 ± 1.06	***		1.59 ± 1.90	
2	3.98 ± 0.62	95.02 ± 3.42	***	5.24 ± 0.28	95.47 ± 6.29	***
3		12.12 ± 1.22	***		9.70 ± 1.06	***
4	4.46 ± 0.72	88.28 ± 5.25	***	4.73 ± 0.40	98.00 ± 4.60	***
LY294002	2.66 ± 0.39	88.30 ± 5.00	***	2.53 ± 0.53	86.71 ± 6.47	***

Percentage of inhibition (Inh.%) at 10 μM. The results are presented as mean ± S.E.M. (n = 3–5). *** *p* < 0.001 compared with the control (DMSO). LY294002 at 10 μM was used as a positive control.

3. Materials and Methods

3.1. General Experimental Procedures

IR spectra were recorded using a Thermo Scientific Nicolet iS5 FT-IR spectrophotometer (Thermo Scientific, Waltham, MA, USA). Optical activities were measured using a JASCO P-1010 polarimeter (JASCO, Tokyo, Japan). NMR spectra were obtained using JEOL ECZ 400S or 600R NMR spectrometers (JEOL, Tokyo, Japan) with CDCl₃ (Sigma-Aldrich, St. Louis, MO, USA) as the deuterated solvent. The detected signals in ¹H and ¹³C NMR were corrected at 7.26 ppm (singlet) and 77.0 ppm (triplet), respectively. The coupling constants (*J*) were converted to Hz. MS data, including ESIMS and HRESIMS, were obtained using a Bruker 7 Tesla solera FTMS system (Bruker, Bremen, Germany). Two types of TLC analyses were performed using aluminum plates coated with Kieselgel 60 F₂₅₄ (0.25 mm) and RP-18 F_{254S} (0.25 mm) (Merck, Darmstadt, Germany). For chromatographic separation, a glass column was used, which was packed with a stationary phase of silica gel 60 (40–63 μm and 63–200 μm, Merck, Darmstadt, Germany). NP-HPLC was conducted using a system consisting of a solvent delivery system (L-7110, Hitachi, Tokyo, Japan) and a preparative packed silica gel column (YMC-Pack SIL, SIL-06, 250 × 20 mm, D. 5–5 μm) (Sigma-Aldrich, St. Louis, MO, USA). RP-HPLC was performed using a system consisting of a solvent delivery system (L-2130, Hitachi, Tokyo, Japan), a PDA detector (L-2455, Hitachi, Tokyo, Japan), and a C₁₈ column (Luna 5 μm, C₁₈(2) 100Å AXIA Packed, 250 × 21.2 mm) (Phenomenex, Torrance, CA, USA).

3.2. Animal Material and Isolation of Compounds

The *Lendenfeldia* sp. specimen was obtained by scuba diving off the coast of Southern Taiwan in April 2019. At the National Museum of Marine Biology & Aquarium, Taiwan, a specimen with a voucher number (specimen No. 2019-04-SP) was deposited. *Lendenfeldia* sp. was taxonomically identified by Prof. Yusheng M. Huang from the National Penghu University of Science and Technology, Taiwan. *Lendenfeldia* sp. was collected (2.9 kg) and freeze-dried. The freeze-dried material (213 g, dry weight) was minced and an extract was prepared using a 1:1 mixture of CH₂Cl₂:MeOH (1 L × 6). The resulting extract underwent liquid–liquid partitioning between EtOAc and H₂O. The obtained EtOAc layer (7.9 g) was further subjected to normal-phase column chromatography. Elution was carried out using a gradient solvent system comprising *n*-hexane, followed by increasing polarity mixtures of *n*-hexane and EtOAc, pure acetone, and finally pure methanol as eluting solvents. This process resulted in the production of 14 sub-fractions labeled A–N. Sub-fraction H underwent reversed-phase chromatography on C₁₈ silica gel, eluted with a MeOH:H₂O mixture (50% MeOH to pure MeOH), and yielded six additional sub-fractions, H1–H6. Sub-fraction H5 then underwent RP-HPLC using an isocratic solvent system of MeOH:H₂O (8:2), resulting in the isolation of compound 2 (1.3 mg). Fraction I was purified using NP-HPLC using a CH₂Cl₂:acetone mixture (4:1) as an isocratic solvent system with a flow

rate of 3.0 mL/min, yielding eight sub-fractions, which were labeled I1–I8. Sub-fraction I5 was further purified using RP-HPLC with an isocratic solvent system of MeOH:H₂O (4:1) at a flow rate of 5 mL/min, resulting in the isolation of compounds **3** (0.9 mg) and **4** (2.1 mg). Similarly, sub-fraction I6 underwent RP-HPLC using an isocratic solvent system of MeOH:H₂O (4:1) at a flow rate of 5 mL/min, leading to the isolation of compound **1** (0.5 mg).

Lendenfedarane R (**1**): Amorphous powder; $[\alpha]_D^{25} +21$ (c 0.025, CHCl₃); IR (ATR) ν_{\max} 3429, 1736, 1703 cm⁻¹; ESIMS m/z 469 [M + Na]⁺; HRESIMS m/z 469.29256 [M + Na]⁺ (calcd. for C₂₇H₄₂O₅ + Na, 469.29245); ¹H (400 MHz, CDCl₃) and ¹³C (100 MHz, CDCl₃) NMR spectroscopic data.

Lendenfedarane S (**2**): Amorphous powder; $[\alpha]_D^{25} +61$ (c 0.025, CHCl₃); IR (ATR) ν_{\max} 3417, 1707, 1676 cm⁻¹; ESIMS m/z 425 [M + Na]⁺; HRESIMS m/z 425.26645 [M + Na]⁺ (calcd. for C₂₅H₃₈O₄ + Na, 425.26623); ¹H (600 MHz, CDCl₃) and ¹³C (150 MHz, CDCl₃) NMR spectroscopic data.

Lendenfedarane T (**3**): Amorphous powder; $[\alpha]_D^{25} +40$ (c 0.045, CHCl₃); IR (ATR) ν_{\max} 3459, 1727, 1666 cm⁻¹; ESIMS m/z 485 [M + Na]⁺; HRESIMS m/z 485.28737 [M + Na]⁺ (calcd. for C₂₇H₄₂O₆ + Na, 485.28736); ¹H (400 MHz, CDCl₃) and ¹³C (100 MHz, CDCl₃) NMR spectroscopic data.

Lendenfedarane U (**4**): Amorphous powder; $[\alpha]_D^{25} +76$ (c 0.105, CHCl₃); IR (ATR) ν_{\max} 3486, 1726, 1655 cm⁻¹; ESIMS m/z 469 [M + Na]⁺; HRESIMS m/z 469.29221 [M + Na]⁺ (calcd. for C₂₇H₄₂O₅ + Na, 469.28736); ¹H (600 MHz, CDCl₃) and ¹³C (150 MHz, CDCl₃) NMR spectroscopic data.

3.3. In Silico Calculations

To minimize molecular energy, the molecular structures were optimized at the MM2 level, resulting in the generation of a mol file. This mol file was analyzed using the MMFF94 force field in GaussView 6.1 (Gaussian Inc., Wallingford, CT, USA) with the assistance of the GMMX package, which allowed us to explore the conformational search results. The obtained data were imported into Gaussian 16 software (Gaussian Inc., Wallingford, CT, USA). In Gaussian 16, the structures underwent further optimization using the time-dependent density functional theory (TDDFT) methodology. The optimization was conducted in the solvent phase using the PCM/mpw1pw91/6-31 g(d,p) levels, enabling GIAO-DFT calculation. In the final step, the computed NMR results were averaged, taking into consideration the proportion of each conformer [49].

3.4. Preparation of Human Neutrophils

Blood samples were collected via venipuncture from human donors aged between 20 and 30 years. The Institutional Review Board (IRB) of Chang Gung Memorial Hospital approved and oversaw the protocol, which was identified as IRB No. 202002493A3. Neutrophil purification was performed using a previously established technique [7]. The process involved several steps, including hypotonic lysis, dextran sedimentation, and separation of erythrocytes using a Ficoll Hypaque gradient. Once the human neutrophils were isolated, they were placed in a 50 mL centrifuge tube containing an HBSS buffer solution devoid of calcium (Ca²⁺) and magnesium (Mg²⁺). The pH of the solution was adjusted to 7.4, and the viability of the neutrophils was assessed using the trypan blue exclusion method to ensure that more than 98% of the cells remained viable. Subsequently, the neutrophils were examined in HBSS with 1 mM CaCl₂ at a temperature of 37 °C.

3.5. Measurement of Superoxide Anion (O₂^{•-}) Generation

The evaluation of O₂^{•-} generation involved the utilization of ferricytochrome *c* and the inhibitory effect of superoxide dismutase (SOD) on its reduction process [15]. After adding ferricytochrome *c* (0.6 mg/mL), neutrophils at a concentration of 6 × 10⁵ cells/mL were equilibrated at 37 °C and incubated for 5 min. Subsequently, the neutrophils were treated with either pure compounds or DMSO (0.1% as a control). To enhance the reaction,

cytochalasin B (CB) was introduced at a concentration of 1 $\mu\text{g}/\text{mL}$ [7]. The activated mixture was then incubated for 3 min after stimulation with 0.1 μM fMLF. The reduction of ferricytochrome *c* was continuously monitored at 550 nm by measuring absorbance changes using a spectrophotometer (U-3010, Hitachi, Tokyo, Japan).

3.6. Measurement of Elastase Release

To evaluate the degranulation of azurophilic granules, an elastase release assay was conducted using MeO-Suc-Ala-Ala-Pro-Val-p-nitroanilide as the substrate for elastase [7]. Neutrophils (6×10^5 cells/mL) were equilibrated at 37 °C after the addition of MeO-Suc-Ala-Ala-Pro-Val-p-nitroanilide (100 μM). The cells were then incubated for 5 min before treatment with pure compounds. To enhance the reaction, CB (0.5 g/mL) was added, followed by the introduction of fMLF (0.1 μM) to induce cellular activation. Elastase release was assessed by continuously monitoring changes in absorbance at 405 nm.

3.7. Statistics

Statistical calculations were performed using Student's *t*-test (GraphPad Software 9.0.2, San Diego, CA, USA). A significance level of $p < 0.05$ was employed to determine statistical significance.

4. Conclusions

In this study, we identified and characterized four new 24-homoscalarane compounds, lendenfeldaranes R–U (1–4), isolated from *Lendenfeldia* sp. through comprehensive chromatographic and spectroscopic analyses. The structures, relative stereochemistry, and absolute configurations of these compounds were determined. The *in vitro* assays demonstrated that compounds possessing C-17-18-24-conjugated functionality exhibited significant inhibitory effects on key inflammatory responses, including the generation of superoxide anions and the release of elastase in human neutrophils. Our findings showed that *Lendenfeldia* sp. is an excellent source of anti-inflammatory agents with unique structures that can be further developed into potential drug leads.

Supplementary Materials: The following supporting information can be downloaded at: <https://www.mdpi.com/article/10.3390/ph16091258/s1>, Figure S1: IR spectrum of compound 1; Figure S2: ESIMS spectrum of compound 1; Figure S3: HRESIMS spectrum of compound 1; Figure S4: ^1H -NMR spectrum (400 MHz) of compound 1 in CDCl_3 ; Figure S5: ^{13}C NMR spectrum (100 MHz) of compound 1 in CDCl_3 ; Figure S6: HSQC spectrum of compound 1 in CDCl_3 ; Figure S7: HMBC spectrum of compound 1 in CDCl_3 ; Figure S8: ^1H - ^1H COSY spectrum of compound 1 in CDCl_3 ; Figure S9: NOESY spectrum of compound 1 in CDCl_3 ; Figure S10: IR spectrum of compound 2; Figure S11: ESIMS spectrum of compound 2; Figure S12: HRESIMS spectrum of compound 2; Figure S13: ^1H NMR spectrum (600 MHz) of compound 2 in CDCl_3 ; Figure S14: ^{13}C NMR spectrum (100 MHz) of compound 2 in CDCl_3 ; Figure S15: HSQC spectrum of compound 2 in CDCl_3 ; Figure S16: HMBC spectrum of compound 2 in CDCl_3 ; Figure S17: ^1H - ^1H COSY spectrum of compound 2 in CDCl_3 ; Figure S18: NOESY spectrum of compound 2 in CDCl_3 ; Figure S19: IR spectrum of compound 3; Figure S20: ESIMS spectrum of compound 3; Figure S21: HRESIMS spectrum of compound 3; Figure S22: ^1H NMR spectrum (400 MHz) of compound 3 in CDCl_3 ; Figure S23: ^{13}C NMR spectrum (100 MHz) of compound 3 in CDCl_3 ; Figure S24: DEPT spectrum of compound 3 in CDCl_3 ; Figure S25: HSQC spectrum of compound 3 in CDCl_3 ; Figure S26: HMBC spectrum of compound 3 in CDCl_3 ; Figure S27: ^1H - ^1H COSY spectrum of compound 3 in CDCl_3 ; Figure S28: NOESY spectrum of compound 3 in CDCl_3 ; Figure S29: IR spectrum of compound 4; Figure S30: ESIMS spectrum of compound 4; Figure S31: HRESIMS spectrum of compound 4; Figure S32: ^1H NMR spectrum (600 MHz) of compound 4 in CDCl_3 ; Figure S33: ^{13}C NMR spectrum (150 MHz) of compound 4 in CDCl_3 ; Figure S34: HSQC spectrum of compound 4 in CDCl_3 ; Figure S35: HMBC spectrum of compound 4 in CDCl_3 ; Figure S36: ^1H - ^1H COSY spectrum of compound 4 in CDCl_3 ; Figure S37: NOESY spectrum of compound 4 in CDCl_3 .

Author Contributions: The experiments were conceived and designed by B.-R.P., K.-H.L. and P.-J.S. Sample collections, extraction, isolation, and structure determination were performed by B.-R.P., L.-G.Z. and L.-Y.C. T.-L.H. and K.-H.L. conducted the pharmacological experiments. J.-H.S., T.-L.H., K.-H.L. and P.-J.S. contributed reagents and analysis tools. Data interpretation, manuscript writing, and paper revision were carried out by B.-R.P., M.E.-S., M.-H.L., K.-H.L. and P.-J.S. All authors have read and agreed to the published version of the manuscript.

Funding: This research received primary support from grants awarded to P.-J.S. from the National Museum of Marine Biology & Aquarium and the National Science and Technology Council (Grant Nos MOST 109-2320-B-291-001-MY3 and 111-2320-B-291-001), Taiwan. Additional support was provided by grants from the National Science and Technology Council (MOST 110-2320-B-038-034, MOST 111-2320-B-038-040-MY3; MOST 111-2321-B-255-001), Ministry of Education (DP2-110-21121-01-N-12-03), and Taipei Medical University (TMU109-AE1-B15) awarded to K.-H. L. The authors express their gratitude for all the funding received.

Institutional Review Board Statement: The study adhered to the principles outlined in the Declaration of Helsinki and received approval from the Institutional Review Board (IRB) at Chang Gung Memorial Hospital. The protocol for studies involving human participants was assigned the code No. 202002493A3.

Informed Consent Statement: Informed consent was obtained from all subjects involved in the study.

Data Availability Statement: Data is contained within the article and Supplementary Material.

Acknowledgments: The authors express their gratitude to Hsiao-Ching Yu and Chao-Lien Ho from the High Valued Instrument Center, National Sun Yat-Sen University, for providing the mass (MS 006500) and NMR (NMR 001100) spectra (NSTC 112-2740-M-110-002).

Conflicts of Interest: The authors declare no conflict of interest.

References

- Galitz, A.; Cook, S.d.C.; Ekins, M.; Hooper, J.N.; Naumann, P.T.; De Voogd, N.J.; Wahab, M.A.; Wörheide, G.; Erpenbeck, D. Identification of an aquaculture poriferan “Pest with Potential” and its phylogenetic implications. *Peer J* **2018**, *6*, e5586. [[CrossRef](#)]
- Alvi, K.; Crews, P. Homoscalarane sesterterpenes from *Lendenfeldia frondosa*. *J. Nat. Prod.* **1992**, *55*, 859–865. [[CrossRef](#)] [[PubMed](#)]
- Chill, L.; Rudi, A.; Akin, M.; Loya, S.; Hizi, A.; Kashman, Y. New sesterterpenes from Madagascan *Lendenfeldia* sponges. *Tetrahedron* **2004**, *60*, 10619–10626. [[CrossRef](#)]
- Kazlauskas, R.; Murphy, P.; Wells, R. Five new C26 tetracyclic terpenes from a sponge (*Lendenfeldia* sp.). *Aust. J. Chem.* **1982**, *35*, 51–59. [[CrossRef](#)]
- Peng, B.-R.; Lai, K.-H.; Chang, Y.-C.; Chen, Y.-Y.; Su, J.-H.; Huang, Y.M.; Chen, P.-J.; Yu, S.S.-F.; Duh, C.-Y.; Sung, P.-J. Sponge-derived 24-homoscalaranes as potent anti-inflammatory agents. *Mar. Drugs* **2020**, *18*, 434. [[CrossRef](#)] [[PubMed](#)]
- Peng, B.-R.; Lai, K.-H.; Chen, Y.-Y.; Su, J.-H.; Huang, Y.M.; Chen, Y.-H.; Lu, M.-C.; Yu, S.S.-F.; Duh, C.-Y.; Sung, P.-J. Probing anti-proliferative 24-homoscalaranes from a sponge *Lendenfeldia* sp. *Mar. Drugs* **2020**, *18*, 76. [[CrossRef](#)]
- Peng, B.-R.; Lai, K.-H.; Lee, G.-H.; Yu, S.S.-F.; Duh, C.-Y.; Su, J.-H.; Zheng, L.-G.; Hwang, T.-L.; Sung, P.-J. Scalarane-type sesterterpenoids from the marine sponge *Lendenfeldia* sp. alleviate inflammation in human neutrophils. *Mar. Drugs* **2021**, *19*, 561. [[CrossRef](#)]
- Sera, Y.; Adachi, K.; Shizuri, Y. A new epidioxy sterol as an antifouling substance from a Palauan marine sponge, *Lendenfeldia chondrodes*. *J. Nat. Prod.* **1999**, *62*, 152–154. [[CrossRef](#)]
- Dai, J.; Liu, Y.; Zhou, Y.-D.; Nagle, D.G. Cytotoxic metabolites from an Indonesian sponge *Lendenfeldia* sp. *J. Nat. Prod.* **2007**, *70*, 1824–1826. [[CrossRef](#)]
- Alahdal, A.M.; Asfour, H.Z.; Ahmed, S.A.; Noor, A.O.; Al-Abd, A.M.; Elfaky, M.A.; Elhady, S.S. Anti-helicobacter, antitubercular and cytotoxic activities of scalaranes from the red sea sponge *Hyrtios erectus*. *Molecules* **2018**, *23*, 978. [[CrossRef](#)]
- Cao, F.; Wu, Z.-H.; Shao, C.-L.; Pang, S.; Liang, X.-Y.; de Voogd, N.J.; Wang, C.-Y. Cytotoxic scalarane sesterterpenoids from the South China Sea sponge *Carteriospongia foliascens*. *Org. Biomol. Chem.* **2015**, *13*, 4016–4024. [[CrossRef](#)] [[PubMed](#)]
- Elhady, S.S.; Al-Abd, A.M.; El-Halawany, A.M.; Alahdal, A.M.; Hassanean, H.A.; Ahmed, S.A. Antiproliferative scalarane-based metabolites from the Red Sea sponge *Hyrtios erectus*. *Mar. Drugs* **2016**, *14*, 130. [[CrossRef](#)] [[PubMed](#)]
- Elhady, S.S.; El-Halawany, A.M.; Alahdal, A.M.; Hassanean, H.A.; Ahmed, S.A. A new bioactive metabolite isolated from the Red Sea marine sponge *Hyrtios erectus*. *Molecules* **2016**, *21*, 82. [[CrossRef](#)] [[PubMed](#)]
- Hahn, D.; Won, D.H.; Mun, B.; Kim, H.; Han, C.; Wang, W.; Chun, T.; Park, S.; Yoon, D.; Choi, H. Cytotoxic scalarane sesterterpenes from a Korean marine sponge *Psammodictyon* sp. *Bioorg. Med. Chem. Lett.* **2013**, *23*, 2336–2339. [[CrossRef](#)]
- Hassan, M.H.; Rateb, M.E.; Hetta, M.; Abdelaziz, T.A.; Sleim, M.A.; Jaspars, M.; Mohammed, R. Scalarane sesterterpenes from the Egyptian Red Sea sponge *Phyllospongia lamellosa*. *Tetrahedron* **2015**, *71*, 577–583. [[CrossRef](#)]

16. Jeon, J.-E.; Bae, J.; Lee, K.J.; Oh, K.-B.; Shin, J. Scalarane sesterterpenes from the sponge *Hyatella* sp. *J. Nat. Prod.* **2011**, *74*, 847–851. [[CrossRef](#)]
17. Kaweetripob, W.; Mahidol, C.; Tuntiwachwuttikul, P.; Ruchirawat, S.; Prawat, H. Cytotoxic sesterterpenes from Thai marine sponge *Hyrtios erectus*. *Mar. Drugs* **2018**, *16*, 474. [[CrossRef](#)]
18. Kwon, O.-S.; Kim, D.; Kim, C.-K.; Sun, J.; Sim, C.J.; Oh, D.-C.; Lee, S.K.; Oh, K.-B.; Shin, J. Cytotoxic scalarane sesterterpenes from the sponge *Hyrtios erectus*. *Mar. Drugs* **2020**, *18*, 253. [[CrossRef](#)]
19. Lai, K.-H.; Liu, Y.-C.; Su, J.-H.; El-Shazly, M.; Wu, C.-F.; Du, Y.-C.; Hsu, Y.-M.; Yang, J.-C.; Weng, M.-K.; Chou, C.-H. Antileukemic scalarane sesterterpenoids and meroditerpenoid from *Carteriospongia (Phyllospongia)* sp., induce apoptosis via dual inhibitory effects on topoisomerase II and Hsp90. *Sci. Rep.* **2016**, *6*, 36170. [[CrossRef](#)]
20. Lee, Y.-J.; Kim, S.-H.; Choi, H.; Lee, H.-S.; Lee, J.-S.; Shin, H.-J.; Lee, J. Cytotoxic furan- and pyrrole-containing scalarane sesterterpenoids isolated from the sponge *Scalariispongia* sp. *Molecules* **2019**, *24*, 840. [[CrossRef](#)]
21. Lu, D.; Luo, X.-C.; Liu, J.; Wu, G.-L.; Yu, Y.; Xu, Y.-N.; Lin, H.-W.; Yang, F. Phyllofolactones NT, bioactive bishomoscalarane sesterterpenoids from the marine sponge *Phyllospongia foliascens*. *Tetrahedron* **2023**, *137*, 133382. [[CrossRef](#)]
22. Shin, A.-Y.; Lee, H.-S.; Lee, J. Isolation of Scalimides A–L: β -alanine-bearing scalarane analogs from the marine sponge *Spongia* sp. *Mar. Drugs* **2022**, *20*, 726. [[CrossRef](#)]
23. Shin, A.-Y.; Son, A.; Choi, C.; Lee, J. Isolation of scalarane-type sesterterpenoids from the marine sponge *Dysidea* sp. and stereochemical reassignment of 12-*epi*-phyllactone D/E. *Mar. Drugs* **2021**, *19*, 627. [[CrossRef](#)] [[PubMed](#)]
24. Su, M.-Z.; Zhang, Q.; Yao, L.-G.; Wu, B.; Guo, Y.-W. Hyrtiosins F and G, two new scalarane sesterterpenes from the South China sea sponge *Hyrtios erecta*. *J. Asian Nat. Prod. Res.* **2022**, *25*, 741–747. [[CrossRef](#)]
25. Tommonaro, G.; De Rosa, S.; Carnuccio, R.; Maiuri, M.C.; De Stefano, D. Marine sponge sesterterpenoids as potent apoptosis-inducing factors in human carcinoma cell lines. In *Handbook of Anticancer Drugs from Marine Origin*; Springer: Cham, Switzerland, 2015; pp. 439–479.
26. Tran, H.N.K.; Kim, M.J.; Lee, Y.-J. Scalarane sesterterpenoids isolated from the marine sponge *Hyrtios erectus* and their Cytotoxicity. *Mar. Drugs* **2022**, *20*, 604. [[CrossRef](#)] [[PubMed](#)]
27. Yang, F.; Gan, J.-H.; Liu, X.-Y.; Lin, H.-W. Scalarane sesterterpenes from the Paracel islands marine sponge *Hyrtios* sp. *Nat. Prod. Commun.* **2014**, *9*, 763–764. [[CrossRef](#)]
28. Yang, I.; Lee, J.; Lee, J.; Hahn, D.; Chin, J.; Won, D.H.; Ko, J.; Choi, H.; Hong, A.; Nam, S.-J. Scalalactams A–D, scalarane sesterterpenes with a γ -lactam moiety from a Korean *Spongia* sp. Marine sponge. *Molecules* **2018**, *23*, 3187. [[CrossRef](#)]
29. Yang, I.; Nam, S.-J.; Kang, H. Two new scalaranes from a Korean marine sponge *Spongia* sp. *Nat. Prod. Sci.* **2015**, *21*, 289–292. [[CrossRef](#)]
30. Yu, H.-B.; Hu, B.; Wu, G.-F.; Ning, Z.; He, Y.; Jiao, B.-H.; Liu, X.-Y.; Lin, H.-W. Phyllospongianes A–E, dinorscalarane sesterterpenes from the marine sponge *Phyllospongia foliascens*. *J. Nat. Prod.* **2023**, *86*, 1754–1760. [[CrossRef](#)]
31. Zhang, H.; Crews, P.; Tenney, K.; Valeriote, F.A. Cytotoxic phyllactone analogs from the marine sponge *Phyllospongia papyracea*. *Med. Chem.* **2017**, *13*, 295–300. [[CrossRef](#)]
32. Chakraborty, K.; Francis, P. Hyrtioscalaranes A and B, two new scalarane-type sesterterpenes from *Hyrtios erectus* with anti-inflammatory and antioxidant effects. *Nat. Prod. Res.* **2021**, *35*, 5559–5570. [[CrossRef](#)] [[PubMed](#)]
33. Francis, P.; Chakraborty, K. Anti-inflammatory scalarane-type sesterterpenes, erectascalaranes A–B, from the marine sponge *Hyrtios erectus* attenuate pro-inflammatory cyclooxygenase-2 and 5-lipoxygenase. *Med. Chem. Res.* **2021**, *30*, 886–896. [[CrossRef](#)]
34. Kikuchi, H.; Tsukitani, Y.; Shimizu, I.; Kobayashi, M.; Kitagawa, I. Foliaspongins, an antiinflammatory bishomosesterterpene from the marine sponge *Phyllospongia foliascens* (Pallas). *Chem. Pharm. Bull.* **1981**, *29*, 1492–1494. [[CrossRef](#)]
35. Kikuchi, H.; Tsukitani, Y.; Shimizu, I.; Kobayashi, M.; Kitagawa, I. Marine natural products. XI. An antiinflammatory scalarane-type bishomosesterterpene, foliaspongins, from the Okinawan marine sponge *Phyllospongia foliascens* (Pallas). *Chem. Pharm. Bull.* **1983**, *31*, 552–556. [[CrossRef](#)]
36. Lee, S.-M.; Kim, N.-H.; Lee, S.; Kim, Y.-N.; Heo, J.-D.; Jeong, E.-J.; Rho, J.-R. Deacetylphyllaketol, a new phyllaketol derivative from a marine sponge, genus *Phyllospongia*, with potent anti-inflammatory activity in in vitro co-culture model of intestine. *Mar. Drugs* **2019**, *17*, 634. [[CrossRef](#)]
37. Chang, L.C.; Otero-Quintero, S.; Nicholas, G.M.; Bewley, C.A. Phyllofolactones A–E: New bishomoscalarane sesterterpenes from the marine sponge *Phyllospongia lamellose*. *Tetrahedron* **2001**, *57*, 5731–5738. [[CrossRef](#)]
38. Choi, J.-H.; Lee, H.-S.; Campos, W.L. Scalarane-type Sesterterpenes from the Philippines Sponge *Hyrtios* sp. *Ocean Polar Res.* **2020**, *42*, 15–20.
39. Daletos, G.; Ancheeva, E.; Chaidir, C.; Kalscheuer, R.; Proksch, P. Antimycobacterial metabolites from marine invertebrates. *Arch. Pharm.* **2016**, *349*, 763–773. [[CrossRef](#)]
40. Hertzner, C.; Kehraus, S.; Böhringer, N.; Kaligis, F.; Bara, R.; Erpenbeck, D.; Wörheide, G.; Schäberle, T.F.; Wägele, H.; König, G.M. Antibacterial scalarane from *Doriprismatica stellata* nudibranchs (Gastropoda, Nudibranchia), egg ribbons, and their dietary sponge *Spongia* cf. *agaricina* (Demospongiae, Dictyoceratida). *Beilstein J. Org. Chem.* **2020**, *16*, 1596–1605. [[CrossRef](#)]
41. Song, J.; Jeong, W.; Wang, N.; Lee, H.-S.; Sim, C.J.; Oh, K.-B.; Shin, J. Scalarane sesterterpenes from the sponge *Smenospongia* sp. *J. Nat. Prod.* **2008**, *71*, 1866–1871. [[CrossRef](#)]
42. Chen, L.Y.; Peng, B.R.; Lai, G.Y.; Weng, H.J.; El-Shazly, M.; Su, C.H.; Su, J.H.; Sung, P.J.; Liao, C.P.; Lai, K.H. Chemometric-guided exploration of marine anti-neurofibroma leads. *Front. Mar. Sci.* **2022**, *9*, 930736. [[CrossRef](#)]

43. Herrero-Cervera, A.; Soehnlein, O.; Kenne, E. Neutrophils in chronic inflammatory diseases. *Cell. Mol. Immunol.* **2022**, *19*, 177–191. [[CrossRef](#)] [[PubMed](#)]
44. Wéra, O.; Lancellotti, P.; Oury, C. The dual role of neutrophils in inflammatory bowel diseases. *J. Clin. Med.* **2016**, *5*, 118. [[CrossRef](#)]
45. Lai, Y.-Y.; Chen, L.-C.; Wu, C.-F.; Lu, M.-C.; Wen, Z.-H.; Wu, T.-Y.; Fang, L.-S.; Wang, L.-H.; Wu, Y.-C.; Sung, P.-J. New cytotoxic 24-homoscalarane sesterterpenoids from the sponge *Ircinia felix*. *Int. J. Mol. Sci.* **2015**, *16*, 21950–21958. [[CrossRef](#)] [[PubMed](#)]
46. Lai, Y.-Y.; Lu, M.-C.; Wang, L.-H.; Chen, J.-J.; Fang, L.-S.; Wu, Y.-C.; Sung, P.-J. New scalarane sesterterpenoids from the Formosan sponge *Ircinia felix*. *Mar. Drugs* **2015**, *13*, 4296–4309. [[CrossRef](#)]
47. Hii, C.S.; Marin, L.A.; Halliday, D.; Robertson, D.M.; Murray, A.W.; Ferrante, A. Regulation of human neutrophil-mediated cartilage proteoglycan degradation by phosphatidylinositol-3-kinase. *Immunology* **2001**, *102*, 59–66. [[CrossRef](#)] [[PubMed](#)]
48. Chen, P.J.; Tseng, H.H.; Wang, Y.H.; Fang, S.Y.; Chen, S.H.; Chen, C.H.; Tsai, S.C.; Chang, Y.C.; Tsai, Y.F.; Hwang, T.L. Palbociclib blocks neutrophilic phosphatidylinositol 3-kinase activity to alleviate psoriasiform dermatitis. *Br. J. Pharmacol.* **2023**, *180*, 2172–2188. [[CrossRef](#)]
49. Grimblat, N.; Zanardi, M.M.; Sarotti, A.M. Beyond DP4: An improved probability for the stereochemical assignment of isomeric compounds using quantum chemical calculations of NMR shifts. *J. Org. Chem.* **2015**, *80*, 12526–12534. [[CrossRef](#)]

Disclaimer/Publisher’s Note: The statements, opinions and data contained in all publications are solely those of the individual author(s) and contributor(s) and not of MDPI and/or the editor(s). MDPI and/or the editor(s) disclaim responsibility for any injury to people or property resulting from any ideas, methods, instructions or products referred to in the content.